*Tellus (2004), 56A, 514–519*
*Printed in UK. All rights reserved*


**TELLUS**

# Model study of soil-moisture influence on precipitation seesaw in the southern United States

*By* JIANJUN XU[2], XIAOGANG GAO[1]* and SOROOSH SOROOSHIAN[1], [1]*Department of Civil and Environmental Engineering, University of California, Irvine, CA 92697-2175, USA;* [2]*Department of Hydrology and Water Resource, University of Arizona, Tucson, AZ 85721, USA*

(Manuscript received 2 September 2003; in final form 22 March 2004)

ABSTRACT

A coupled atmosphere–land-surface mesoscale model is used to assess the responses of precipitation to soil-moisture anomalies in two regions: (1) the core region of the North American Monsoon (NAM; 105°–112°W, 24°–36°N); (2) the central–southern United States (CS-US; 85°–95°W, 30°–36°N). Results from a series of numerical experiments integrated from July to September 2000 show that precipitation increases in the NAM region in July with a prescribed wet soil-moisture anomaly; meanwhile, precipitation decreases in the CS-US region. In the following months, when the prescribed wet soil-moisture anomaly in the NAM region was removed, the increase in precipitation in the NAM region becomes weaker and shifts eastward to the CS-US region. By September, an inverse precipitation seesaw in these two regions is built up. Except for local evaporation, the transportation of atmospheric moisture affects the interaction between soil moisture and precipitation, especially in the regions and periods without the prescribed soil-moisture anomaly. The soil-moisture anomaly in the NAM region is only partially responsible for the precipitation seesaw in the southern United States.

## 1. Introduction

With the appearance of the North American Monsoon (NAM) from July through to September, precipitation increases sharply in the south-western United States and north-western Mexico (Douglas et al., 1993). Meanwhile, precipitation decreases substantially over the central United States (Mock, 1996; Higgins et al., 1998; Xu and Small, 2002). This out-of-phase relationship is referred to as a precipitation seesaw phenomenon. The factors responsible for such a precipitation anomaly can come from many aspects, including atmosphere, ocean and land processes. In this study, we investigate the influence of land processes, basically the influence of soil moisture on the precipitation seesaw over the southern United States.

Soil moisture can strongly influence the overlying atmospheric system, particularly through the exchanges of water and energy between the atmosphere and land surface (Yeh et al., 1984). Soil moisture with a relatively long-term memory or a persistent effect on the surface boundary of the atmosphere can modulate regional and large-scale atmospheric circulation (Kunkel et al., 1994). Previous studies, such as Barnett et al. (1989), have found that the anomalous soil-moisture conditions in one region also influence precipitation in an adjacent region via the effects of the regional or global-scale atmospheric circulation. For the extreme rainfall events in July 1993 over the central United States, a series of numerical studies using the European Centre for Medium-Range Weather Forecast (ECMWF) model (Beljaars et al., 1996; Betts et al., 1999; Viterbo and Betts, 1999) shows that the prediction skill of precipitation in a monthly range is related to the time-scale of soil-moisture sustainability. However, the response of rainfall to soil-moisture variations involves very complicated processes that depend critically on the specific atmosphere and land-surface conditions. For the NAM region (south-western United States and north-western Mexico) with complicated topography (Fig. 1) and heterogeneity of climate, hydrology and biology, it is still unknown how the precipitation seesaw will change when the soil-moisture anomaly suddenly occurs through the monsoon rainfalls in July each year.

A coupled atmosphere–land-surface mesoscale model is used to investigate how the monsoon season soil-moisture anomaly influences precipitation over the southern United States. The model and simulation designs are described in Section 2. The results, analyses and conclusions of the numerical experiments are presented in Sections 3 and 4, respectively.

## 2. Model and simulation designs

The Pennsylvania State University/National Center for Atmospheric Research (PSU/NCAR) fifth-generation mesoscale

*Corresponding author.
e-mail: gaox@uci.edu

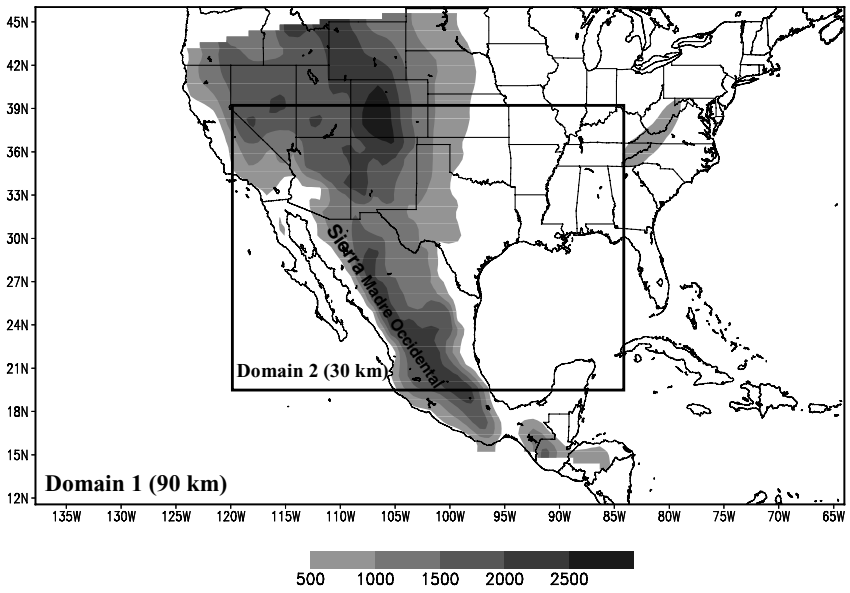


*Fig 1.* Simulation domain. The outside box is a coarse grid (domain 1) in a 90-km distance with 40 × 68 points; the inner box is a nested grid (domain 2) in a 30-km distance with 100 × 70 points. The shaded area indicates topography with heights greater than 500 m.

model (MM5; Grell et al., 1994) coupled to the Oregon State University (OSU) land-surface model (Chen and Dudhia, 2001) was used in this study. Based on our previous study (Xu and Small, 2002), we chose the Grell cumulus convective parametrization and the Rapid Radiation Transfer Model (RRTM) radiation scheme for convection simulation. The planetary boundary layer (PBL) was modeled by the high-resolution Blackadar scheme. In the OSU land-surface model, the land use and land cover at each grid point are clarified by 24 categories (from urban land to snow or ice) and represented by the climatology values of associated physical properties such as albedo, moisture availability, emissivity, roughness length and thermal inertia. These parameter values also vary according to the category and time of year (Grell et al., 1994).

A two-way multigrid system was employed (Fig. 1) which includes a 90-km coarse-grid mesh, covering a large portion of North America and the surrounding oceans and a 30-km nested-grid mesh centered at the core region of the NAM, which allows for a reasonable representation of the complex topography and heterogeneity of the region.

The initial atmospheric and surface fields and the boundary conditions for the coarse domain are taken from the National Center for Atmospheric Research/NCAR (NCEP/NCAR) reanalysis data set (Kalnay et al., 1996). The outer two rows and columns of the domain (domain 1) are specified using the prediction fields from the reanalysis data. The lateral boundary conditions also update with time. The same configuration is applied to the nested domain (domain 2) with its initial and boundary conditions obtained from the parent grid.

Two types of simulations are conducted using the MM5 system: (1) the control run (CTL) driven by the reanalysis data integrated for four months from June 1 to September 30 2000; (2) a series of numerical experiments (EXP) using the same forcing but with prescribed soil-moisture anomalies in the NAM region for the entire month of July to simulate the soil-moisture anomaly resulting from the occurrence of monsoon rainfalls. The prescribed soil-moisture anomalies are calculated based on the climatology of soil moisture from the NCEP/NCAR reanalysis data

$$\theta_{\mathrm{E}}(t, x, y) = F\theta_{\mathrm{C}}(t, x, y).$$

Here, $\theta_{\mathrm{C}}(t, x, y)$ represents the field (as a function of time and space) of mean volumetric soil-moisture content in July 2000 calculated from the control run, $\theta_{\mathrm{E}}(t, x, y)$ is the field used to prescribe the soil-moisture anomaly in the NAM region for the numerical experiments, and $F$ is a factor. In experiment 1 (EXP1), $F$ equals 160%, which is the ratio of soil-moisture climatology (the July mean of reanalysis soil moisture from 1948 to 2000) to the mean of July 2000 in the NAM region. In order to further test the sensitivity of the soil-moisture anomaly, in experiment 2 (EXP2), the values of $F$ are set at 120%, 140%, 180% and 200%, respectively. Notice that the soil moisture is prescribed only in the NAM region and only for the month of July 2000. In August and September, the state of soil moisture in the study region is calculated through the land-surface model with the soil moisture prescribed in July.

## 3. Results

### *3.1. Soil-moisture pattern in the control simulation*

Figure 2 compares the total (0–200 cm) soil-moisture fields ($\theta$) in July–September (JAS) 2000 calculated from the NCEP/NCAR reanalysis data and from the control run. The reanalysis field (Fig. 2a) shows that a large area with $\theta$ less than 0.15 spans the

entire south-western United States, and the areas with relatively high $\theta$ (in excess of 0.20) are located in the southern portion of Mexico and in the central–southern United States (CS-US) region. Compared to the reanalysis field, the field of control simulation shows a similar pattern excluding the areas of central Mexico and southern Texas (Fig. 2b). The cause for the marked differences of soil-moisture fields in central Mexico may be ascribed to the coarse resolution used in the NCEP/NCAR reanalysis. Such coarse resolution may not take into account the terrain complexity in Mexico and is unable to describe the heterogeneity in precipitation and soil moisture. The control run gives us a clue that MM5 should be able to perform a better simulation of the precipitation and soil moisture in the region using high resolution. The soil-moisture field ($\theta$) shows that soil moisture in the NAM region is the driest in the study domain, and the drier soil is located around the NAM region and the wetter soil in the CS-US region. Corresponding to the soil-moisture distribution, the model produces more precipitation in the CS-US region than in the south-western United States during the summer season (not shown).

### 3.2. *Response of precipitation to soil-moisture anomaly*

The numerical experiment (EXP1) is conducted to investigate what happens to the precipitation over the southern United States, if the soil moisture in the NAM region changes sharply. The differences of monthly precipitation between the EXP1 and CTL results (EXP1-CTL) are used to demonstrate the response of precipitation to the prescribed wet soil-moisture anomaly in the NAM region (Fig. 3). In July, with the increase of soil moisture in the NAM region, precipitation increases over most of the NAM region, except over the western hillslope of the Sierra Madre Occidental in coastal northern Mexico (Fig. 1), where precipitation reduces, which shows the high heterogeneity of precipitation in the region. In contrast, precipitation over the CS-US region (85°–95°W, 30°–36°N) is dominated by a negative anomaly. A deeper seesaw pattern of precipitation between the NAM region

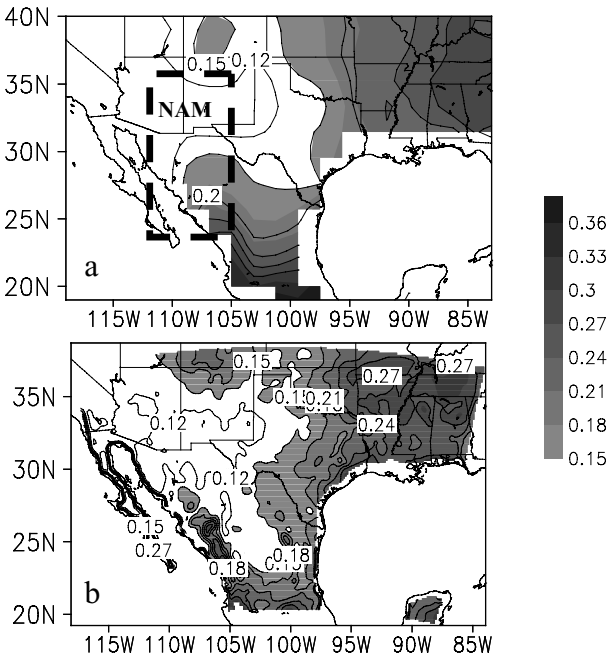


*Fig 2.* Average volumetric soil-moisture content ($\theta$) in the total model layer (0–200 cm) for JAS 2000: (a) NCEP/NCAR reanalysis field; (b) control simulation. The dashed box in the upper panel indicates the prescribed core area of the NAM (105°–112°W, 24°–36°N).

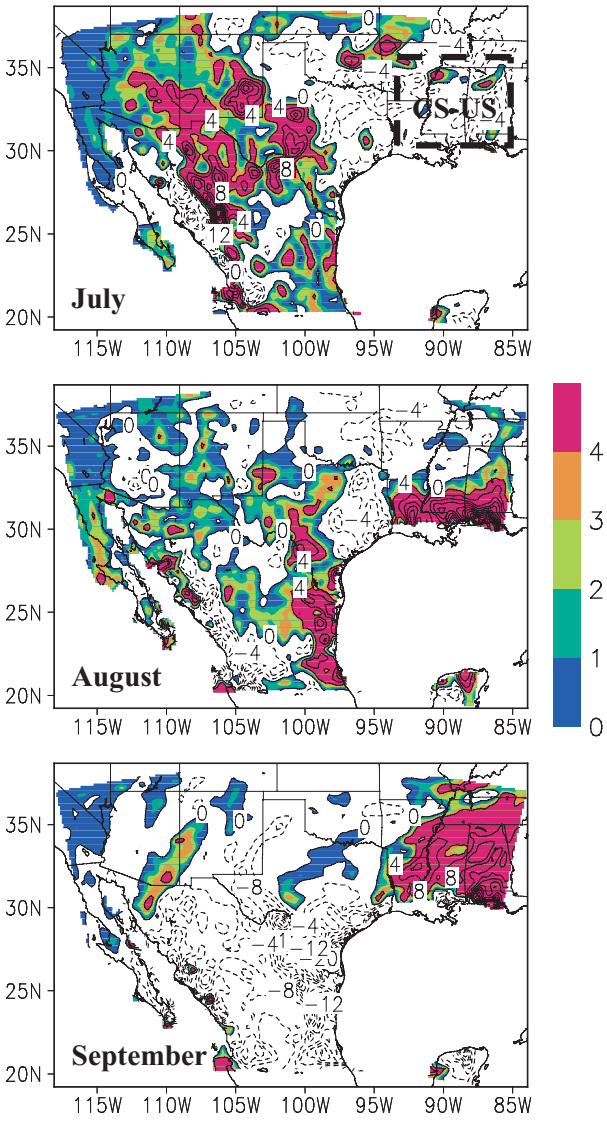


*Fig 3.* Monthly precipitation difference between the anomaly experiment (EXP1) and control run (EXP-CTL) during the summertime: (a) July; (b) August; (c) September. Shaded areas indicate positive value (units are cm mon$^{-1}$).

and the CS-US region is produced because of the prescribed soil-moisture anomaly in the NAM region.

In August, without the prescription of the soil-moisture anomaly, the positive anomaly of precipitation remains over most of the NAM region. It is interesting that a positive anomaly of precipitation appears in the CS-US region at the same time. By September, the positive rainfall anomaly of July in the NAM region has been completely replaced by the negative anomaly, and the negative anomaly of July in the CS-US region changes to the positive one. An inverse phase of the precipitation seesaw occurs in the southern United States.

In summary, model precipitation over the southern United States is highly sensitive to the soil-moisture variation in the NAM region. An increase of rainfall in the NAM region versus a decrease of rainfall in the CS-US region occurs due to the prescribed wet soil moisture in July, which enhances the precipitation seesaw in the southern United States. In the following two months of August and September, when rainfall is decreasing in the NAM region and increasing in the CS-US region, the seesaw phase is reversed.

### *3.3. Processes responsible for the precipitation anomaly*

The question is why can the soil-moisture anomaly in the NAM region affect the precipitation pattern in the southern United States? In general, the generation of summer rainfall relies on two atmospheric conditions: (1) sufficient air moisture content; (2) convective instability. In order to understand the precipitation seesaw in the southern United States, these conditions in the NAM region and the CS-US regions are compared.

*3.3.1. Moisture content.* The moisture content comes mainly from two possible sources: (1) local evaporation; (2) moisture transportation associated with atmospheric circulation. The local evaporation increases with an increase in soil moisture. Figure 4a shows that the evaporation in the NAM region increases remarkably because of the prescribed wet soil-moisture anomaly in July. Afterwards, the positive anomaly reduces in August and September, while Fig. 4b indicates that evaporation remains unchanged in the CS-US region. The moisture transportation is also related to the soil-moisture anomaly. This can be illustrated through the atmosphere moisture balance over the region. The basic components of atmosphere moisture balance include evaporation, precipitation, precipitable water and moisture transportation (i.e. the net moisture flux through the horizontal boundary). With the above discussions about the precipitation and evaporation variations corresponding to the CTL results, the change of precipitable water (Figs. 4c–d ) can be used to explain the moisture transportation over the NAM and CS-US regions. Over the NAM region, because of the prescribed soil-moisture anomaly in July, evaporation increased substantially and it was the major moisture source for the increases in both precipitation and precipitable water (Fig. 4c). Afterwards evaporation reduced with significant rainfall decrease. In September, the precipitable water possesses a relatively strong negative anomaly, which indicates net

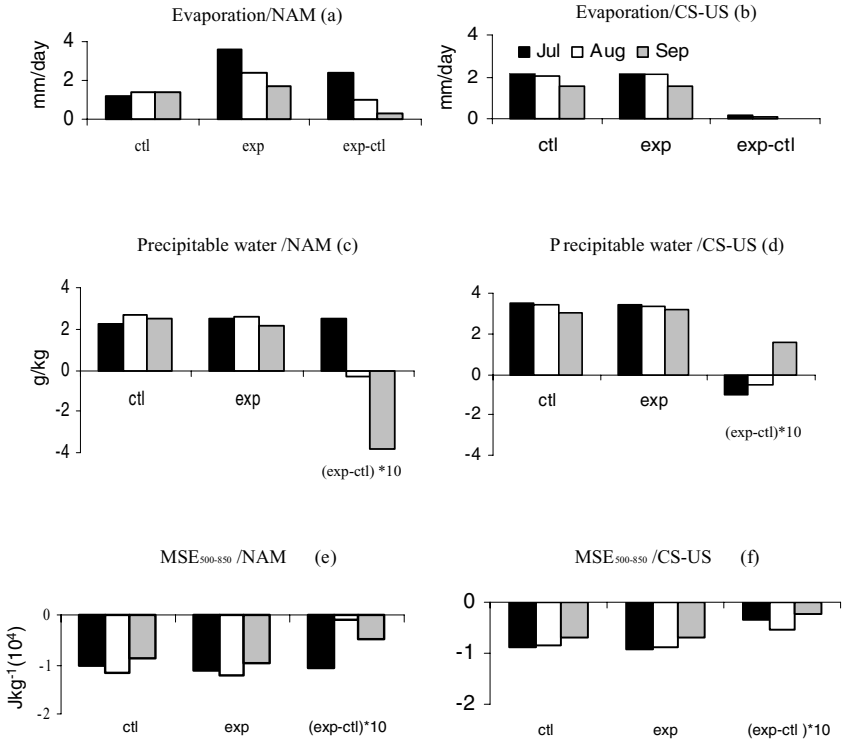


*Fig 4.* Monthly evaporation, precipitable water, and convective instability ($MSE_{500-850}$) in the anomaly experiments and control run over the NAM and the CS-US regions.

moisture transportation out of the region. Over the CS-US region, for the three months, both evaporation and precipitable water show no substantial change. Therefore, the significant rainfall increase in September resulted from the moisture transportation flowing into the region.

It is clear that the soil-moisture anomaly induces the anomalies of atmosphere moisture. However, the response of atmosphere moisture in the NAM and CS-US region to soil-moisture anomaly is different. In July, with the prescribed soil-moisture anomaly, the air-moisture content anomaly in the NAM region results mainly from the local evaporation, but the air-moisture content in the CS-US region comes mainly from the moisture transportation. In September, evaporation continues to affect the air-moisture content in both the NAM and CS-US regions, but the major sources for air-moisture content in both regions are replaced by the moisture transportations associated with atmospheric circulations.

*3.3.2. Convective instability.* For the generation of convective rainfall, convective instability is another necessary condition, except for the air-moisture content. Here, we used the difference of moist static energy (MSE, defined as $CpT + Lq + gz$) at 500 and 850 hPa ($MSE_{500-850}$) to quantify convective instability: $MSE_{500-850} > 0$ represents stable atmosphere and $MSE_{500-850} < 0$ unstable atmosphere. Figures 4e–f show that the atmosphere in the summertime is always unstable in these two regions. This instability becomes stronger when the soil moisture increases, but the strength of instability changes with the period and location. The $MSE_{500-850}$ variations show that the convective instability is the strongest over the NAM region in July, which is consistent with the positive anomaly of precipitation. In addition, the decrease in negative $MSE_{500-850}$ over the CS-US region is smaller than that over the NAM region. Obviously, soil-moisture anomaly modulates the convective instability.

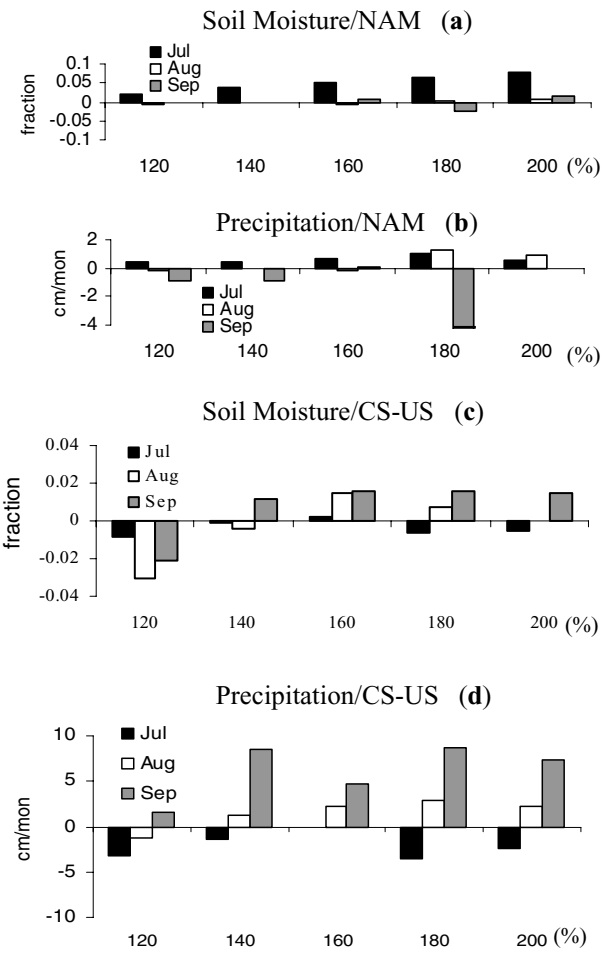


*Fig 5.* Monthly soil-moisture and precipitation difference (EXP-CTL) over the NAM and the CS-US regions change with the prescribed amplitude of the soil-moisture anomaly.

### *3.4. Effect of soil-moisture intensity on precipitation*

To ensure that the influence of soil moisture on the precipitation seesaw is not a single case result and also to understand how the soil moisture intensity influences on precipitation, the relationship between soil-moisture and precipitation anomalies is tested using different $F$ ($F = 120\%, 140\%, 180\%$ and $200\%$) for the prescribed soil moisture in the NAM region in July. Corresponding to these prescribed soil-moisture anomalies (Fig. 5a), the precipitation anomaly in the NAM region is positive in July, negative in September and irregular in August (Fig. 5b). In contrast, soil-moisture and precipitation anomalies in the CS-US region show the opposite anomalies (Figs. 5c–d). The amplitudes of the precipitation anomaly in both domains do not change linearly with the increase in soil moisture in the NAM region. For example, when soil moisture increases from 160% to 180% in July, precipitation in the NAM region reduces dramatically in September, but when soil moisture increases to 200%, no precipitation anomaly occurs in the same region. These results imply that soil moisture does not affect precipitation alone; therefore, the impact on precipitation is non-linear. Other factors related to atmospheric dynamical processes and surface processes may also affect the quantity of the precipitation anomaly. Figure 4 shows that, when soil moisture changes, the atmospheric moisture content and convective instability varies. This displays the complexity of the interaction between the atmosphere and land surface.

## 4. Conclusions

The results of numerical experiments explore the relationship between the monsoon soil-moisture anomaly and the precipitation seesaw in the southern United States. With an increase in soil moisture in the NAM region in July, precipitation in the southern United States shows an enhanced precipitation seesaw with the positive anomaly in the NAM region and the negative anomaly in the CS-US region. Afterwards, the positive

precipitation anomaly moves eastward from the NAM region to the CS-US region; in September, a stronger inverse seesaw pattern sets up over the southern United States. Evaporation in the NAM region in July and atmospheric moisture transportation to the CS-US region in September play an important role in alternatively shifting the moisture convergence from west to east in the southern United States, which provides the condition for the inverse of the precipitation seesaw.

Recent studies (Roads et al., 1999; Lenters et al., 2000; Heck et al., 2001; Kanamitsu et al., 2002) have indicated that the NCEP/NCAR reanalysis data of soil moisture contain large uncertainties, such as overestimating the yearly soil-moisture cycle in some regions and underestimating interannual variability due to its relaxation to climatology. The quality of mesoscale simulations and predictions can be affected significantly by those uncertainties; therefore, further model studies and field measurements for soil moisture and its impact on the atmospheric system are important.

## 5. Acknowledgments

The authors would like to thank the NCAR Scientific Computing Division (SCD) for supporting part of the calculation and providing the reanalysis and global sea surface temperature (SST) data, and the Climate Prediction Center (CPC) for providing the real-time precipitation analysis data. The comments and suggestions offered by the two anonymous reviewers contributed to considerable improvements of the paper. This study is partially sponsored by the National Aeronautics and Space Administration (NASA) grant NAG5-11044, the National Oceanic and Atmospheric Administration (NOAA) grant NA16GP1605, and the NSF/SAHRA ('Sustainability of semi-arid Hydrology and Riparian Areas') grant ERA-9876800.

## References

Barnett, T. P., Dumenil, L., Schlese, U., Roeckner, E. and Latif, M. 1989. Effects of Eurasian snow cover on regional and global climate variations. *J. Atmos. Sci.* **46**, 661–685.

Beljaars, A. C. M., Viterbo, P., Miller, M. J. and Betts, A. K. 1996. The anomalous rainfall over the United States during July 1993: sensitivity to land surface parameterization and soil moisture anomalies. *Mon. Wea. Rev.* **124**, 362–383.

Betts, A. K., Ball, J. H. and Viterbo, P. 1999. Basin-scale surface water and energy budgets for the Mississippi from the ECMWF reanalysis. *JGR-Atmospheres* **104**, D16, 19 293–19 306.

Chen, F. and Dudhia, J. 2001. Coupling an advanced land-surface/hydrology model with the Penn State/NCAR MM5 modeling system. part I: model description and implementation. *Mon. Wea. Rev.* **129**, 569–585.

Douglas, M. W., Maddox, R. A., Howard, K. W. and Reyes, S. 1993. The Mexican monsoon. *J. Climate* **6**, 1665–1677.

Grell, G. A., Dudhia, J. and Stauffer, D. R. 1994. A description of the fifth-generation Penn State/NCAR mesoscale model (MM5). *NCAR Technical Note*, NCAR/TN-398+STR, 117 pp.

Heck, P., Lüthi, D., Wernli, H. and Schär, C. 2001. Climate impacts of European-scale anthropogenic vegetation changes: a sensitivity study using a regional climate model. *JGR-Atmospheres* **106** (D8), 7817–7835.

Higgins, R. W., Mo, K. C. and Yao, Y. 1998. Interannual variability of the U.S. summer precipitation regime with emphasis on the southwestern monsoon. *J. Climate* **11**, 2582–2606

Kalnay, E., Kanamitsu, M., Kistler, R., Collins, W., Deaven, D. et al. 1996. The NCEP/NCAR 40-year reanalysis project. *Bull. Am. Meteorol. Soc.* **77**, 437–471.

Kanamitsu, M., Ebisuzaki, W., Woolen, J., Potter, J. and Fiorino, M. 2002. Overview of NCEP/DOE reanalysis-2. Document available at http://dss.ucar.edu/datasets/ds091.0/docs/ncep-docs/r2sumshort.pdf.

Kunkel, K. E., Changnon, S. A. and Angel, J. R. 1994. Climatic aspects of the 1993 upper Mississippi river basin flood. *Bull. Am. Meteorol. Soc.* **75**, 811–822.

Lenters, J. D., Coe, M. T. and Foley, J. A. 2000. Surface water balance of the continental United States, 1963–1995: regional evaluation of a terrestrial biosphere model and NCEP/NCAR reanalysis. *JGR-Atmospheres* **105** (D17), 22 393–22 425.

Mock, C. J. 1996. Climate controls and spatial variations of precipitation in the western United States. *J. Climate*, **9**, 1111–1125.

Roads, J. O., Chen, S. C., Kanamitsu, M. and Juang, H. 1999. Surface water characteristics in NCEP global spectral model and reanalysis. *JGR-Atmospheres* **104** (D16), 19 307–19 327.

Viterbo, P. and Betts, A. K. 1999. Impact of the ECMWF reanalysis soil water on forecasts of the July 1993 Mississippi flood. *JGR-Atmospheres* **104**, (D16), 19 361–19 366.

Xu, J. J. and Small, E. E. 2002. Simulating summertime rainfall variability in the North American monsoon region: the influence of convection and radiation parameterizations. *JGR-Atmospheres* **107** (D23), 10.1029/2001JD002047.

Yeh, T.-C., Wetherald, R. T. and Manabe, S. 1984. The effect of soil moisture on the short-term climate and hydrology change—a numerical experiment. *Mon. Wea. Rev.* **112**, 474–490.